

UNCLASSIFIED

AD 273 992

*Reproduced
by the*

**ARMED SERVICES TECHNICAL INFORMATION AGENCY
ARLINGTON HALL STATION
ARLINGTON 12, VIRGINIA**



UNCLASSIFIED

NOTICE: When government or other drawings, specifications or other data are used for any purpose other than in connection with a definitely related government procurement operation, the U. S. Government thereby incurs no responsibility, nor any obligation whatsoever; and the fact that the Government may have formulated, furnished, or in any way supplied the said drawings, specifications, or other data is not to be regarded by implication or otherwise as in any manner licensing the holder or any other person or corporation, or conveying any rights or permission to manufacture, use or sell any patented invention that may in any way be related thereto.

273 992

CATALOGED BY ASTIA
AS AD NO. _____

273992

APGC-TDR-62-19

Difference Scheme for Axisymmetric Impact Problem

(Quarterly Progress Report No. 4,
November 3, 1961 - February 3, 1962)

ASTIA
RECEIVED
APR 9 1962
62-3-1
TISIA

Technical Documentary Report No. APGC-TDR-62-19

MARCH 1962

DEPUTY FOR AEROSPACE
AIR PROVING GROUND CENTER
Air Force Systems Command
United States Air Force
Eglin Air Force Base, Florida



Project No. 9860

819 485

(Prepared under Contract No. AF 08(635)-1713 by T.D.Riney, Space Sciences Laboratory,
General Electric Co., Valley Forge Space Technology Center, King of Prussia, Pa.)

Qualified requesters may obtain copies from ASTIA. Orders will be expedited if placed through the librarian or other person designated to request documents from ASTIA.

When US Government drawings, specifications, or other data are used for any purpose other than a definitely related government procurement operation, the government thereby incurs no responsibility nor any obligation whatsoever; and the fact that the government may have formulated, furnished, or in any way supplied the said drawings, specifications, or other data is not to be regarded by implication or otherwise, as in any manner licensing the holder or any other person or corporation, or conveying any rights or permission to manufacture, use, or sell any patented invention that may in any way be related thereto.

FOREWORD

This report was prepared by the Space Sciences Laboratory of the General Electric Missile and Space Vehicle Department under Air Force Contract No. AF 08(635)-1713, Project No. 9860. The contract was monitored by the Ballistics Directorate, APGC (PGWR), Eglin Air Force Base, with Mr. Andrew Bilek as Project Engineer.

ABSTRACT

A numerical scheme which has been successfully employed for two-dimensional hydrodynamics is extended to the axisymmetric visco-plastic equations governing the hypervelocity impact phenomenon. Computing procedures are outlined which are complete enough for interior regions of the medium. The formulation must be further developed, however, to allow for such contingencies as free boundaries, interior empty cells and the axis of symmetry before a computing code can be written for the impact problem.

PUBLICATION REVIEW

This technical documentary report has been reviewed and is approved.



MORRILL E. MARSTON

Colonel, USAF

Deputy for Aerospace

LIST OF SYMBOLS

τ_0	dynamic yield value of shear stress
μ_0	viscosity factor
ρ_0	mass density of undisturbed visco-plastic medium
ρ	density of visco-plastic medium
v_0	impact velocity of projectile
D^2	strain rate invariant
$\mu = \mu(D)$	strain rate dependent viscosity coefficient
τ_{ik}	components of stress tensor
r^2	von Mises flow statistic
t	time
(r, θ, z)	cylindrical coordinates
$\bar{u} = (u, o, v)$	velocity of flow of medium in Eulerian coordinates
p	thermodynamic pressure
I	specific internal energy
e	sum of specific kinetic and internal energies
δr	size of radial space mesh
δz	size of axial space mesh
δt	size of time space mesh
$H = 2d \delta r$	diameter of projectile

$L = l \delta_2$	length of projectile
P, Q	functions with dimensions of stress
k	number of particles initially in each cell
M	total mass of particles in cell
(r_ν, z_ν)	coordinates of ν -th particle
R	total radial momentum in cell
Z	total axial momentum in cell
E	total energy in cell
(\sim)	result of Phase I calculation for ()
$()'$	result of Phase II calculation for ()

TABLE OF CONTENTS

	Page
INTRODUCTION	1
THE PIC FORMULATION	2
(a) Phase I Calculations	3
(b) Phase II Calculations	7
(c) Phase III Calculations	10
CONCLUSIONS	11
BIBLIOGRAPHY	12
APPENDIX A	13
APPENDIX B	15

INTRODUCTION

The object of this theoretical investigation of the hypervelocity impact phenomenon is the solution of the governing equations for the axisymmetric case depicted in Figure 1. The pertinent viscoplastic equations were presented in an earlier report (Ref. 1). Numerical schemes have been developed and solutions obtained for the one-dimensional, time dependent, formulation of the equations (Refs. 2, 3); the results have been amplified in other discussions (Refs. 4, 5). The axisymmetric problem, however, requires the solution of the two-dimensional, time dependent equations. A large difference exists in the difficulty between the 1-D and 2-D problems.

In developing a finite difference formulation of the axisymmetric impact problem, extension of an existing scheme devised for two-dimensional hydrodynamics can be attempted for expediency. Several methods of treatment have been used for those problems dependent upon two or more space coordinates. These variations usually employ (a) Lagrangian coordinates in which the mesh of cells is imbedded in the medium and moves with it (Refs. 6, 7, 8), (b) Eulerian coordinates which are not fixed in the medium but are usually stationary in the laboratory frame of reference, or (c) a mixed Euler-Lagrange system which attempts to take advantage of the better features of both fixed and moveable coordinates (Refs. 9, 10).

The difficulties with schemes employing Lagrangian coordinates is the large distortions which are involved in the present problem. The Eulerian systems have the disadvantage that to account for the projectile-target interface and the free surfaces of the projectile and target is extremely difficult. These are the basic reasons for the decision to adopt the particle-in-cell method (abbreviated PIC) which has been developed at Los Alamos by Dr. Francis H. Harlow and his colleagues.

The essential features of the method have been described in two Los Alamos reports (Refs. 9, 10). Briefly, the space occupied by the medium is divided into a suitably chosen mesh of fixed cells through which the medium moves. The medium within

each cell is represented by a set of mass points (particles). At the end of the n -th time cycle the mass (equal to the sum of the masses of the particles located in that cell) velocity, pressure, and specific internal energy are associated with each cell. To obtain the corresponding data at the end of the $(n + 1)$ -st time cycle one makes a three phase calculation. In Phase I the field functions are changed neglecting the motion of the medium. In Phase II the mass points are moved and the field functions then recalculated to account for the motion. In Phase III various functionals are computed which furnish checks on the accuracy of the calculations.

THE PIC FORMULATION

The projectile is considered to be a circular cylinder of length L and diameter H . The space net size is δr by δz as depicted in Figure 2. For example, the projectile is divided into $\ell \times d$ cells,

$$(1) \quad \ell = L/\delta z \qquad d = H/2\delta r$$

each of which is actually a toroid of revolution. The cells are labeled with index $\binom{j}{i}$, with i and j increasing in the r and z directions, respectively:

$$(2) \quad \text{cell} \binom{j}{i} = \left\{ \begin{array}{l} (i-1)\delta r \leq r < i\delta r \\ (j-1)\delta z \leq z < j\delta z \end{array} \right\}$$

The pressure for cell $\binom{j}{i}$ is p_i^j ; the average pressure along the boundary between cells $\binom{j}{i}$ and $\binom{j}{i+1}$ is denoted by $p_{i+1/2}^j$; while the average pressure between cells $\binom{j}{i}$ and $\binom{j+1}{i}$ is $p_i^{j+1/2}$. Analogous notations are used for the other cell-wise quantities.

Having a different mass for different mass particles is convenient in cylindrical coordinates. Each particle is given a fixed mass whose value is proportional to the radius of the cell within which it lies originally ($t=0$). If there are originally k particles in each cell, then the mass of each of the k particles originally in cell $\binom{j}{i}$ is

$$(3) \quad \frac{2 \pi r_i^j \delta r \delta z \rho_0}{k} = \frac{2 \pi (i - 1/2) (\delta r)^2 \delta z \rho_0}{k}$$

The k particles are assumed to be originally randomly distributed in the cell. The location of each particle at the end of the n - th time cycle is stored in the machine memory until its location at the end of the $(n + 1)$ -st cycle is computed. The conservation of mass is therefore automatic in the PIC method.

(a) Phase I Calculations

The particles are not moved; thus the transport terms are dropped from the momenta and energy equations governing the visco-plastic model (see Appendix A). The tentative new cellwise velocity components and specific internal energy become:

$$(4) \quad \begin{aligned} \tilde{u}_i^j = u_i^j + \frac{2 \pi r_i^j \delta z \delta t}{M_i^j} & \left\{ P_{i+1/2}^j - P_{i-1/2}^j + \frac{2}{\delta r} \left[\mu_{i+1/2}^j (u_{i+1}^j - u_i^j) \right. \right. \\ & \left. \left. - \mu_{i-1/2}^j (u_i^j - u_{i-1}^j) \right] \right\} \\ & + \mu_i^j \frac{4 \pi r_i^j \delta z \delta t}{M_i^j} \left\{ \left(\frac{u}{r} \right)_{i+1/2}^j - \left(\frac{u}{r} \right)_{i-1/2}^j \right\} \\ & + \frac{2 \pi r_i^j \delta r \delta t}{M_i^j} \left\{ Q_i^{j+1/2} - Q_i^{j-1/2} \right\} \end{aligned}$$

$$(5) \quad \begin{aligned} \tilde{v}_i^j = v_i^j + \frac{2 \pi r_i^j \delta r \delta t}{M_i^j} & \left\{ P_{i+1/2}^{j+1/2} - P_{i-1/2}^{j-1/2} + \frac{2}{\delta z} \left[\mu_{i+1/2}^{j+1/2} (v_{i+1}^{j+1} - v_i^j) \right. \right. \\ & \left. \left. - \mu_{i-1/2}^{j-1/2} (v_i^j - v_{i-1}^{j-1}) \right] \right\} \\ & + \frac{2 \pi \delta z \delta t}{M_i^j} \left\{ (rQ)_{i+1/2}^j - (rQ)_{i-1/2}^j \right\} \end{aligned}$$

$$\begin{aligned}
\tilde{I}_i^j &= I_i^j + \frac{1}{2} \left[(u_i^j)^2 + (v_i^j)^2 - (\tilde{u}_i^j)^2 - (\tilde{v}_i^j)^2 \right] \\
&+ \frac{2\pi \delta z \delta t}{M_i^j} \left\{ (P_{ur})_{i+1/2}^j - (P_{ur})_{i-1/2}^j + (Q_{vr})_{i+1/2}^j \right. \\
&- (Q_{vr})_{i-1/2}^j + \frac{(r\mu)_{i+1/2}^j}{\delta r} \left((u_{i+1}^j)^2 - (u_i^j)^2 \right) \\
&- \left. \frac{(r\mu)_{i-1/2}^j}{\delta r} \left((u_i^j)^2 - (u_{i-1}^j)^2 \right) \right\} \\
&+ \frac{2\pi r_i^j \delta r \delta t}{M_i^j} \left\{ (P_v)_{i+1/2}^{j+1/2} - (P_v)_i^{j-1/2} + (Q_u)_i^{j+1/2} \right. \\
&- (Q_u)_i^{j-1/2} + \frac{\mu_i^{j+1/2}}{\delta z} \left((v_i^{j+1})^2 - (v_i^j)^2 \right) \\
&- \left. \frac{\mu_i^{j-1/2}}{\delta z} \left((v_i^j)^2 - (v_{i-1}^j)^2 \right) \right\}
\end{aligned}$$

(6)

where

$$(7) \quad (\text{div } \bar{u})_i^j = \frac{u_{i+1/2}^j - u_{i-1/2}^j}{\delta r} + \left(\frac{u}{r}\right)_i^j + \frac{v_{i+1/2}^j - v_{i-1/2}^j}{\delta z}$$

$$(8) \quad (D^2)_i^j = \left[\frac{u_{i+1/2}^j - u_{i-1/2}^j}{\delta z} + \frac{v_{i+1/2}^j - v_{i-1/2}^j}{\delta r} \right]^2 + 2 \left\{ \left[\frac{u_{i+1/2}^j - u_{i-1/2}^j}{\delta r} \right]^2 + \left[\left(\frac{u}{r}\right)_i^j \right]^2 + \left[\frac{v_{i+1/2}^j - v_{i-1/2}^j}{\delta z} \right]^2 \right\} - \frac{2}{3} \left[(\text{div } \bar{u})_i^j \right]^2$$

$$(9) \quad \mu_i^j = \mu_o + \frac{r_o}{\sqrt{(D^2)_i^j}}$$

$$(10) \quad P_i^j = -p_i^j - \frac{2}{3} \mu_i^j (\text{div } \bar{u})_i^j$$

$$Q_i^j = \mu_i^j \left\{ \frac{u_{i+1/2}^j - u_{i-1/2}^j}{\delta z} + \frac{v_{i+1/2}^j - v_{i-1/2}^j}{\delta r} \right\}$$

$$(11) \quad (\tau^2)_i^j = r_o^2 + 2\mu_o r_o \sqrt{(D^2)_i^j} + \mu_o^2 (D^2)_i^j.$$

At the end of the n - th cycle there are stored in the memory the mass, specific internal energy, velocity components, and the pressure for every cell. Table I shows these together with the quantities which replace them during the sequence of computational steps required for Phase I of the (n + 1) - st time cycle calculations:

Step 1.1 The velocity components at the end of the n - th time cycle are evaluated at the cell boundaries:

$$(12) \quad u_{i-1/2}^j = \frac{u_{i-1}^j + u_i^j}{2} \quad u_i^{j-1/2} = \frac{u_i^{j-1} + u_i^j}{2}$$

$$(13) \quad v_{i-1/2}^j = \frac{v_{i-1}^j + v_i^j}{2} \quad v_i^{j-1/2} = \frac{v_i^{j-1} + v_i^j}{2}$$

Step 1.2 The divergence of the velocity at the cell center is computed using equation (7).

Step 1.3 The value at the cell center of the distortional strain-rate invariant is computed using equation (8).

Step 1.4 The value at the cell center of the strain-rate dependent viscosity coefficient is computed using equation (9).

Step 1.5 The cell center values of the quantities P and Q are computed using equations (10).

Step 1.6 Equation (11) is used to compute the cell center value of the flow statistic. Further, the boundary values of P, Q and μ are computed according to

$$(14) \quad P_{i-1/2}^j = \frac{P_{i-1}^j + P_i^j}{2} \quad . \quad P_i^{j-1/2} = \frac{P_i^{j-1} + P_i^j}{2}$$

$$(15) \quad Q_{i-1/2}^j = \frac{Q_{i-1}^j + Q_i^j}{2} \quad Q_i^{j-1/2} = \frac{Q_i^{j-1} + Q_i^j}{2}$$

$$(16) \quad \mu_{i-1/2}^j = \frac{\mu_{i-1}^j + \mu_i^j}{2} \quad \mu_i^{j-1/2} = \frac{\mu_i^{j-1} + \mu_i^j}{2}$$

Step 1.7 The tentative new cellwise velocity components are now computed using equations (4) and (5).

Step 1.8 The tentative new specific internal energy is computed using equation (6).

Each of these computational steps are made for every cell in the mesh before the subsequent step is made for any one cell. This is necessary since results of the step for cell A are usually required to compute the next step in the cells neighboring A.

(b) Phase II Calculations

At the end of Phase I the tentative values, \tilde{u}, \tilde{v} and \tilde{I} are known for each cell. The mass particles are now moved and this effect is taken into account in recomputing these quantities in the steps depicted in Table II and detailed below.

Step 2.1 This is a preparatory step in which the tentative energy and momentum are totaled over all the particles in the cell at the end of Phase I:

$$(17) \quad \tilde{E}_i^j = M_i^j \left\{ \tilde{T}_i^j + \frac{1}{2} \left[(\tilde{u}_i^j)^2 + (\tilde{v}_i^j)^2 \right] \right\}$$

$$(18) \quad \tilde{R}_i^j = M_i^j \tilde{u}_i^j$$

$$(19) \quad \tilde{Z}_i^j = M_i^j \tilde{v}_i^j$$

Step 2.2 None of the cellwise quantities are changed in this computation; the mass particles are moved. If r_ν, z_ν are the coordinates of a mass particle at the end of the n-th time cycle, its new coordinates are given by

$$(20) \quad \begin{aligned} r'_\nu &= r_\nu + u_\nu \delta t \\ z'_\nu &= z_\nu + v_\nu \delta t \end{aligned}$$

where u_ν and v_ν are computed by the "area averaging" formulas presented in Appendix B. For each mass particle the corresponding coordinates r'_ν, z'_ν replace (r_ν, z_ν) in the machine memory.

Step 2.3 The total mass of the particles in each cell is recomputed to adjust for net loss or gain in the mass present in the cell after the motion of the particles. New values for the new cellwise total energy and new values for the components of the total cellwise momentum are also computed.

$$(21) \quad M_i^{j'} = M_i^j - \sum_{\text{out}} m_\nu + \sum_N \left(\sum_{\text{in}} m_{\nu, N} \right)$$

$$(22) \quad E_i^{j'} = \tilde{E}_i^j - \frac{\tilde{E}_i^j}{M_i^j} \sum_{\text{out}} m_\nu + \sum_N \left(\frac{\tilde{E}_N}{M_N} \sum_{\text{in}} m_{\nu, N} \right)$$

$$(23) \quad R_i^{j'} = \tilde{R}_i^j - \tilde{u}_i^j \sum_{\text{out}} m_\nu + \sum_N \left(\tilde{u}_N \sum_{\text{in}} m_{\nu, N} \right)$$

$$(24) \quad Z_i^{j'} = \tilde{Z}_i^j - \tilde{v}_i^j \sum_{\text{out}} m_\nu + \sum_N \left(\tilde{v}_N \sum_{\text{in}} m_{\nu, N} \right)$$

Here "out" means that the summation is taken over all particles leaving cell $\binom{j}{i}$, N means the summation is taken over all the eight nearest neighbors of cell $\binom{j}{i}$ and the "in" means the mass summation is taken over all particles entering cell $\binom{j}{i}$ from a given neighboring cell N. Only the eight nearest neighbors are considered since δt is restricted to satisfy condition (B-1).

Step 2.4 The cellwise density and the velocity components at the end of the $(n + 1)$ -st time cycle are computed:

$$(25) \quad \rho_i^{j'} = \frac{M_i^{j'}}{2 \pi \delta r \delta z r_i^j}$$

$$(26) \quad u_i^{j'} = R_i^{j'} / M_i^{j'}$$

$$(27) \quad v_i^{j'} = Z_i^{j'} / M_i^{j'}$$

Step 2.5 The cellwise specific internal energy at the end of $(n + 1)$ -st time cycle is computed:

$$(28) \quad I_i^{j'} = \frac{E_i^{j'}}{M_i^{j'}} - \frac{1}{2} \left[\left(u_i^{j'} \right)^2 + \left(v_i^{j'} \right)^2 \right]$$

Step 2.6 The pressure at the end of the $(n + 1)$ -st time cycle is computed:

$$(29) \quad p_i^{j'} = f(\rho_i^{j'}, I_i^{j'})$$

At the end of Step 2.6 the information in the machine memory is in such a form that the computations for the $(n + 2)$ -nd time cycle may begin immediately. However, first making some subsidiary calculations is helpful.

(c) Phase III Calculations

Before proceeding to the next time cycle, computation of the total energy and the components of total momentum is useful. Thus, in the present problem, the total momentum components should be rigorously conserved, but the total energy of the system should be a monotone decreasing function of the time. Set

$$(30) \quad R_{tot.} = \sum_{System} R_i^j \qquad R'_{tot.} = \sum_{System} R_i^j$$

$$(31) \quad Z_{tot.} = \sum_{System} Z_i^j \qquad Z'_{tot.} = \sum_{System} Z_i^{j'}$$

$$(32) \quad E_{tot.} = \sum_{System} E_i^j \qquad E'_{tot.} = \sum_{System} E_i^{j'}$$

where the summation is extended over all cells containing mass particles disturbed during the motion. The restrictions on the momentum and energy then become

$$(33) \quad R'_{tot.} \cong R_{tot.}$$

$$(34) \quad Z'_{\text{tot}} = Z_{\text{tot.}} = \frac{\pi}{4} H^2 L \rho_o v_o$$

$$(35) \quad E'_{\text{tot.}} = E_{\text{tot.}} = \frac{\pi}{8} H^2 L \rho_o v_o^2.$$

CONCLUSIONS

In applying equations (4), (5) and (6) in Step 1.1 the values of velocity and specific internal energy must be known in neighboring cells as well as in the cell in question. Specifically, to calculate \tilde{u}_i^j and \tilde{v}_i^j the pressure and velocity components at the cell centers and boundaries depicted in Figure 3 must be known. The usual computational procedure therefore does not apply near a free surface nor in the vicinity of the axis of symmetry. Another necessary step is to provide for such contingencies as empty cells since the usual scheme also fails for that situation.

Current effort is directed toward devising means for handling these special situations. It is too early to report on these techniques in detail; it should be possible to do so in the next Quarterly Report. Before the actual programming for the IBM 7090 is commenced we intend to visit Dr. Harlow at Los Alamos to discuss the scheme in detail.

BIBLIOGRAPHY

1. Riney, T.D., "A Visco-Plastic Model for Hypervelocity Impact", First Quarterly Report, Contract AF 08(635)-1713, November 3, 1960-February 3, 1961, (APGC-TN-61-16).
2. Riney, T.D., "Study of Equations Governing the Visco-Plastic Model", Second Quarterly Report, Contract AF 08(635)-1713, February 3, 1961-May 3, 1961, (APGC-TN-61-30).
3. Riney, T.D., "Numerical Investigation of One-Dimensional Visco-Plastic Model", Third Quarterly Report, Contract AF 08(635)-1713, May 3, 1961-September 3, 1961.
4. Riney, T.D., and Chernoff, P.R., "Inertial, Viscous, and Plastic Effects in High Speed Impact", Paper presented at the Fifth Symposium on Hypervelocity Impact in Denver, Colorado, October 31, 1961.
5. Riney, T.D., "Theory of High Speed Impact", Final Report, Contract AF 08(635)-1713, December, 1961.
6. Kolsky, H.G., "A Method for the Numerical Solution of Transient Hydrodynamic Shock Problems in Two Space Dimensions", Los Alamos Scientific Laboratory, LA-1867, April 1955.
7. Orlow, T., Piacesi, D. and Sternberg, H.M., "A Computer Program for the Analysis of Transient, Axially Symmetric, Explosion and Shock Dynamics Problems", Naval Ordnance Laboratory, NAVWEPS Report 7265, December, 1960.
8. Goad, W.B., "A Numerical Method for Two-Dimensional Unsteady Fluid Flow", Los Alamos Scientific Laboratory LAMS-2365, November 1960.
9. Evans, M.W., and Harlow, F.H., "The Particle-in-Cell Method for Hydrodynamic Calculations", Los Alamos Scientific Laboratory, LA-2139, November, 1957.
10. Harlow, F.H., "Two-Dimensional Hydrodynamic Calculations", Los Alamos Scientific Laboratory, LA-2301, September, 1959.

APPENDIX A

Let ρ , p , $\bar{u} = (u, 0, v)$ and I denote the density, pressure, velocity and specific internal energy respectively. Then the axisymmetric formulation of the visco-plastic equations may be written in the form (Ref. 1):

$$(A-1) \quad \frac{\partial \rho}{\partial t} + u \frac{\partial \rho}{\partial r} + v \frac{\partial \rho}{\partial z} + \rho \operatorname{div} \bar{u} = 0$$

$$(A-2) \quad \rho \left(\frac{\partial u}{\partial t} + u \frac{\partial u}{\partial r} + v \frac{\partial u}{\partial z} \right) = \frac{\partial}{\partial r} \left(P + 2 \mu (D) \frac{\partial u}{\partial r} \right) + 2 \mu (D) \frac{\partial}{\partial r} \left(\frac{u}{r} \right) + \frac{\partial Q}{\partial z}$$

$$(A-3) \quad \rho \left(\frac{\partial v}{\partial t} + u \frac{\partial v}{\partial r} + v \frac{\partial v}{\partial z} \right) = \frac{\partial}{\partial z} \left(P + 2 \mu (D) \frac{\partial v}{\partial z} \right) + \frac{1}{r} \frac{\partial}{\partial r} (r Q)$$

$$(A-4) \quad \rho \left(\frac{\partial e}{\partial t} + u \frac{\partial e}{\partial r} + v \frac{\partial e}{\partial z} \right) = \frac{1}{r} \frac{\partial}{\partial r} \left\{ r \left[u P + v Q + \mu (D) \frac{\partial}{\partial r} u^2 \right] \right\} + \frac{\partial}{\partial z} \left\{ v P + u Q + \mu (D) \frac{\partial}{\partial z} v^2 \right\}$$

$$(A-5) \quad p = f(\rho, I)$$

where

$$(A-6) \quad \left\{ \begin{array}{l} e = I + \frac{1}{2} (u^2 + v^2) \\ P = -p - \frac{2}{3} \mu (D) \operatorname{div} \bar{u} \\ Q = \mu (D) \left(\frac{\partial u}{\partial z} + \frac{\partial v}{\partial r} \right) \\ \mu (D) = \mu_o + \frac{\tau_o}{\sqrt{D^2}} \\ D^2 = \left(\frac{\partial u}{\partial z} + \frac{\partial v}{\partial r} \right)^2 + 2 \left[\left(\frac{\partial u}{\partial r} \right)^2 + \left(\frac{u}{r} \right)^2 + \left(\frac{\partial v}{\partial z} \right)^2 \right] - \frac{2}{3} (\operatorname{div} \bar{u})^2 \\ \operatorname{div} \bar{u} = \frac{\partial u}{\partial r} + \frac{u}{r} + \frac{\partial v}{\partial z} \end{array} \right.$$

The components of the stress tensor are given by

$$(A-7) \quad \left\{ \begin{array}{l} \tau_{rr} = P + 2 \mu (D) \frac{\partial u}{\partial r} \\ \tau_{\theta\theta} = P + 2 \mu (D) \frac{u}{r} \\ \tau_{zz} = P + 2 \mu (D) \frac{\partial v}{\partial z} \end{array} \right. \quad \tau_{rz} = Q$$

and the flow criterion is given in terms of

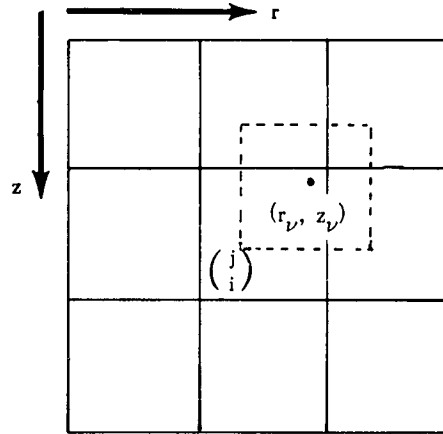
$$(A-8) \quad \tau^2 = \tau_o^2 + 2 \mu_o \tau_o \sqrt{D^2} + \mu_o^2 D^2.$$

APPENDIX B

Consider a particle in cell $\begin{pmatrix} j \\ i \end{pmatrix}$. During the $(n + 1)$ -st time cycle it may remain in that cell or it may move into one of the eight nearest neighbor cells. No other possibility exists since we restrict δt to satisfy the inequalities

$$(B-1) \quad \delta t u_{\max} < \delta r \qquad \delta t v_{\max} < \delta z .$$

Imagine a rectangle of cell size located about each particle, the particle being at the center (see sketch). The effective velocity for moving the particle is taken as the weighted average of the four cellwise velocities of the cell that the superposed rectangle overlaps. The weightings are proportional to the overlap areas.



The cells which the superposed rectangle overlaps vary with the quadrant of cell $\begin{pmatrix} j \\ i \end{pmatrix}$ within which the particle lies. The possibilities and corresponding effective velocity components of the particle are as follows:

First Quadrant

$$\left\{ \begin{array}{l} (i - 1/2) \delta r \leq r_\nu < i \delta r \\ (j - 1) \delta z \leq z_\nu < (j - 1/2) \delta z \end{array} \right\}$$

$$(B-2) \quad u_\nu = \frac{1}{\delta r \delta z} \left\{ \begin{array}{l} [(j - 1/2) \delta z - z_\nu] \left([r_\nu - (i - 1/2) \delta r] u_{i+1}^{j-1} \right. \\ \left. + [(i + 1/2) \delta r - r_\nu] u_i^{j-1} \right) + [z_\nu - (j - 3/2) \delta z] \left([(i + 1/2) \delta r - r_\nu] u_i^j \right. \\ \left. + [r_\nu - (i - 1/2) \delta r] u_{i+1}^j \right) \end{array} \right\}$$

$$(B-3) \quad v_\nu = \frac{1}{\delta r \delta z} \left\{ \begin{array}{l} [(j - 1/2) \delta z - z_\nu] \left([r_\nu - (i - 1/2) \delta r] v_{i+1}^{j-1} + [(i + 1/2) \delta r - r_\nu] v_i^{j-1} \right) \\ + [z_\nu - (j - 3/2) \delta z] \left([(i + 1/2) \delta r - r_\nu] v_i^j + [r_\nu - (i - 1/2) \delta r] v_{i+1}^j \right) \end{array} \right\}$$

Second Quadrant

$$\left\{ \begin{array}{l} (i - 1) \delta r \leq r_\nu < (i - 1/2) \delta r \\ (j - 1) \delta z \leq z_\nu < (j - 1/2) \delta z \end{array} \right\}$$

$$(B-4) \quad u_\nu = \frac{1}{\delta r \delta z} \left\{ \begin{array}{l} [(j - 1/2) \delta z - z_\nu] \left([r_\nu - (i - 3/2) \delta r] u_i^{j-1} + [(i - 1/2) \delta r - r_\nu] u_{i-1}^{j-1} \right) \\ + [z_\nu - (j - 3/2) \delta z] \left([(i - 1/2) \delta r - r_\nu] u_{i-1}^j + [r_\nu - (i - 3/2) \delta r] u_i^j \right) \end{array} \right\}$$

$$(B-5) \quad v_\nu = \frac{1}{\delta r \delta z} \left\{ \left[(j - 1/2) \delta z - z_\nu \right] \left(\left[r_\nu - (i - 3/2) \delta r \right] v_i^{j-1} + \left[(i - 1/2) \delta r - r_\nu \right] v_{i-1}^{j-1} \right) \right. \\ \left. + \left[z_\nu - (j - 3/2) \delta z \right] \left(\left[(i - 1/2) \delta r - r_\nu \right] v_{i-1}^j + \left[r_\nu - (i - 3/2) \delta r \right] v_i^j \right) \right\}$$

Third Quadrant

$$\left\{ \begin{array}{l} (i - 1) \delta r \leq r_\nu < (i - 1/2) \delta r \\ (j - 1/2) \delta z \leq z_\nu < j \delta z \end{array} \right\}$$

$$(B-6) \quad u_\nu = \frac{1}{\delta r \delta z} \left\{ \left[(j + 1/2) \delta z - z_\nu \right] \left(\left[r_\nu - (i - 3/2) \delta r \right] u_i^j + \left[(i - 1/2) \delta r - r_\nu \right] u_{i-1}^j \right) \right. \\ \left. + \left[z_\nu - (j - 1/2) \delta z \right] \left(\left[(i - 1/2) \delta r - r_\nu \right] u_{i-1}^{j+1} + \left[r_\nu - (i - 3/2) \delta r \right] u_i^{j+1} \right) \right\}$$

$$(B-7) \quad v_\nu = \frac{1}{\delta r \delta z} \left\{ \left[(j + 1/2) \delta z - z_\nu \right] \left(\left[r_\nu - (i - 3/2) \delta r \right] v_i^j + \left[(i - 1/2) \delta r - r_\nu \right] v_{i-1}^j \right) \right. \\ \left. + \left[z_\nu - (j - 1/2) \delta z \right] \left(\left[(i - 1/2) \delta r - r_\nu \right] v_{i-1}^{j+1} + \left[r_\nu - (i - 3/2) \delta r \right] v_i^{j+1} \right) \right\}$$

Fourth Quadrant

$$\left\{ \begin{array}{l} (i - 1/2) \delta r \leq r_\nu < i \delta r \\ (j - 1/2) \delta z \leq z_\nu < j \delta z \end{array} \right\}$$

$$(B-8) \quad u_\nu = \frac{1}{\delta r \delta z} \left\{ \begin{array}{l} [(j + 1/2) \delta z - z_\nu] \left([r_\nu - (i - 1/2) \delta r] u_{i+1}^j + [(i + 1/2) \delta r - r_\nu] u_i^j \right) \\ + [z_\nu - (j - 1/2) \delta z] \left([(i + 1/2) \delta r - r_\nu] u_i^{j+1} + [r_\nu - (i - 1/2) \delta r] u_{i+1}^{j+1} \right) \end{array} \right\}$$

$$(B-9) \quad v_\nu = \frac{1}{\delta r \delta z} \left\{ \begin{array}{l} [(j + 1/2) \delta z - z_\nu] \left([r_\nu - (i - 1/2) \delta r] v_{i+1}^j + [(i + 1/2) \delta r - r_\nu] v_i^j \right) \\ + [z_\nu - (j - 1/2) \delta z] \left([(i + 1/2) \delta r - r_\nu] v_i^{j+1} + [r_\nu - (i - 1/2) \delta r] v_{i+1}^{j+1} \right) \end{array} \right\}$$

TABLE II

Sequence of storage changes for cell (j) during Phase II.
 The dash indicates that the information stored in that
 cell is not used in subsequent calculations.

	v_1^j	u_1^j	\bar{u}_1^j	\bar{v}_1^j	v_1^j	u_1^j	\bar{u}_1^j	\bar{v}_1^j	v_1^j	u_1^j	\bar{u}_1^j	\bar{v}_1^j	v_1^j	u_1^j	\bar{u}_1^j	\bar{v}_1^j	v_1^j	u_1^j	\bar{u}_1^j	\bar{v}_1^j	
2.1	—	—	—	—	—	—	—	—	—	—	—	—	—	—	—	—	—	—	—	—	—
2.2	—	\bar{r}_1^j	\bar{z}_1^j	\bar{e}_1^j	—	—	—	—	—	—	—	—	—	—	—	—	—	—	—	—	—
2.3	—	—	—	—	—	—	—	—	—	—	—	—	—	—	—	—	—	—	—	—	—
2.4	—	\bar{r}_1^j	\bar{z}_1^j	\bar{e}_1^j	—	—	—	—	—	—	—	—	—	—	—	—	—	—	—	—	—
2.5	—	—	—	—	—	—	—	—	—	—	—	—	—	—	—	—	—	—	—	—	—
2.6	—	\bar{r}_1^j	\bar{z}_1^j	\bar{e}_1^j	—	—	—	—	—	—	—	—	—	—	—	—	—	—	—	—	—

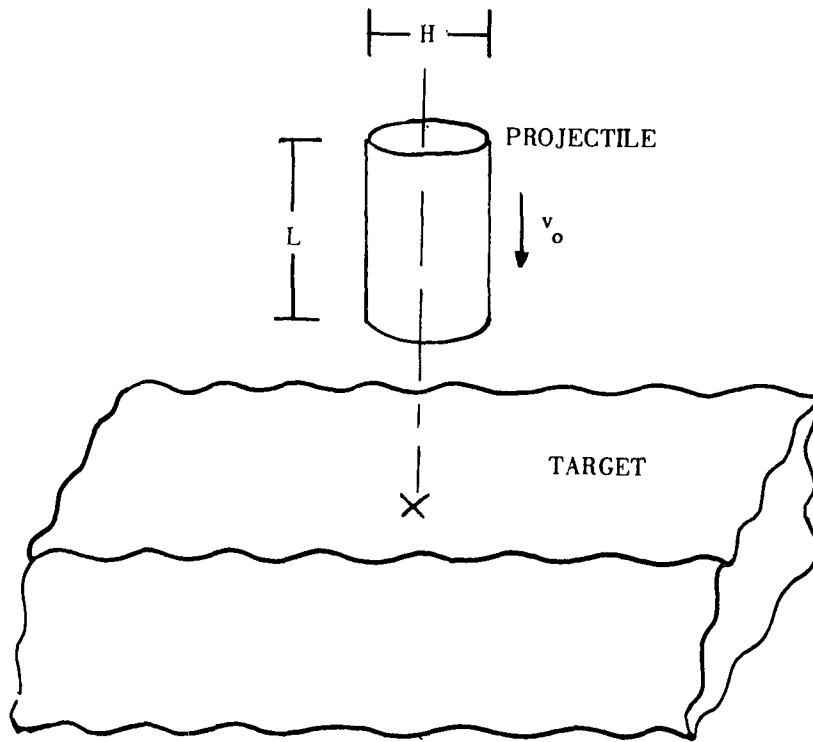


Figure 1. Illustration of projectile-target configuration just before impact.

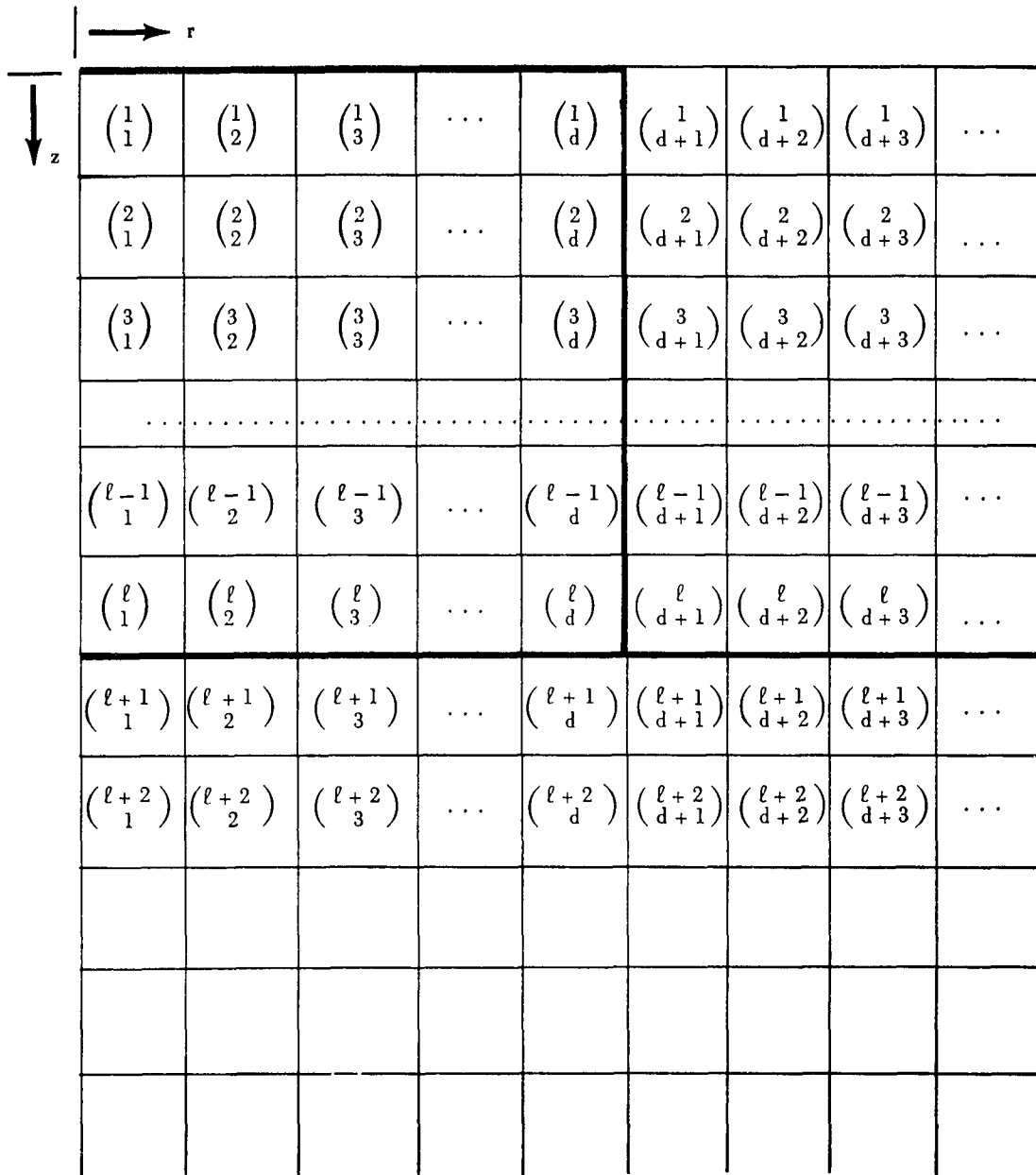


Figure 2. Space mesh cells of PIC method superposed over the projectile-target configuration at time $t = 0$.

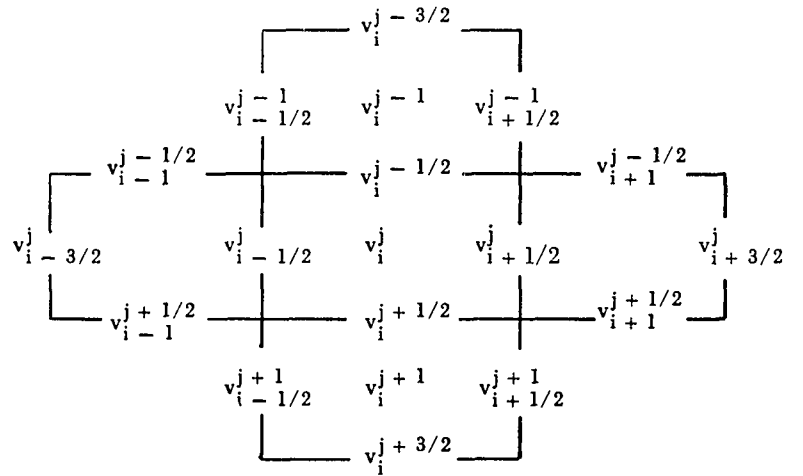
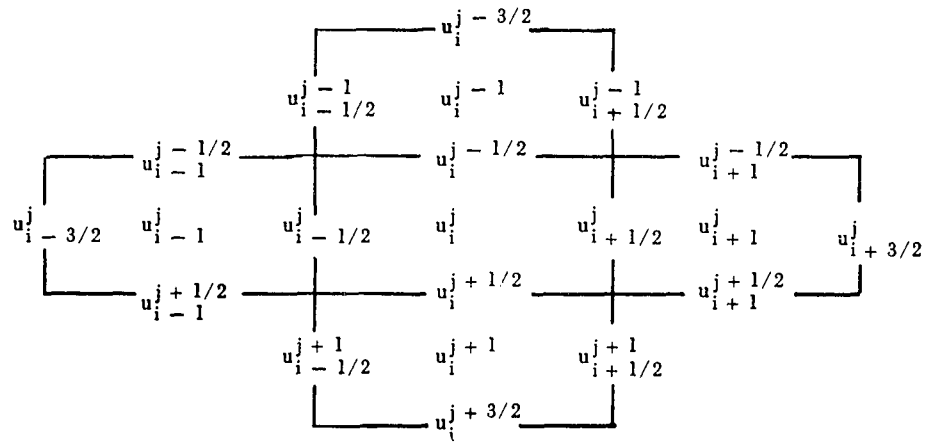
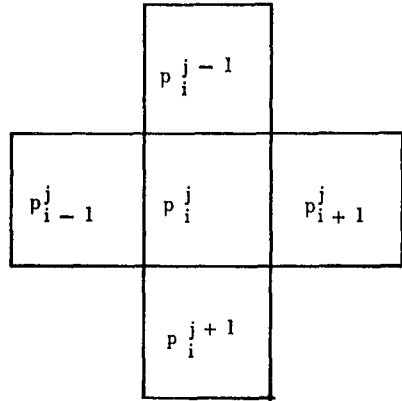


Figure 3. Layout depicting the quantities required to compute tentative values of \tilde{u}_i^j , \tilde{v}_i^j and \tilde{f}_i^j .

INITIAL DISTRIBUTION

2	Wpns Sys Eval Gp	1	NOL (Ballistics Dept)
2	Hq USAF (AFDAP/W-AD)	2	Nav Wpns Lab (Tech Lib)
2	Hq USAF (AFDRD-ER-1)	2	Ames Rsch Ctr (Lib)
2	ASD (ASRCEP-1)	2	Ames Rsch Ctr (High Speed
2	ASD (ASRNGW)		Rsch Div)
2	AFSWC	2	Lewis Rsch Ctr
2	OAR	2	Applied Rsch Lab (JHU)
2	OAR (RROSA)	1	Armour Rsch Foundation
2	BSD	1	Franklin Institute (Lib)
2	SSD	1	Franklin Institute
1	AFCRL	1	Jet Propulsion Lab
2	AU	1	USAF Proj RAND
1	TAC (TPL-RQD-M)	1	University of Chicago
2	Langley Rsch Ctr (Lib)	30	ASTIA (TIPCR)
2	NASA (Code 9262)		APGC
2	Springfield Armory (R&D Div)	2	ASQR
2	Watervliet Arsenal (ORDBR-R)	2	PGAPI
2	ARO (Scientific Info Br)	3	PGEH
2	ABMA (ORDAB-HT)	2	PGWR
2	Watertown Arsenal	2	PGW
2	Picatinny Arsenal (ORDBB-TH8)	40	PGWRT
1	CofOrd (ORDTB)		
1	CofOrd (ORDTM)		
1	CofOrd (ORDTS)		
1	BRL (Free-Flight Aero Br)		
1	BRL (Exter Ballistics Lab)		
1	BRL (Tech Info Br)		
1	BRL (Dev & Proff Svcs)		
1	ARGMA (ORDDW-IDE)		
1	Frankford Arsenal (Lib)		
1	Frankford Arsenal (Pitman-Dunn Lab)		
1	Rock Island Arsenal		
2	NOTS (Code 5007)		
2	NOTS (Tech Lib)		
1	BUWEPS (R-12)		
3	BUWEPS (RM)		
1	BUWEPS (RM-3)		
1	BUWEPS (RMGA-41)		
1	BUWEPS (RT-1)(J. D. N.)		
1	BUWEPS (RMMO-4)		
1	NOL (Assoc Dir/Aeroballistics)		
1	NOL (Aerodynamics Dept)		

Air Proving Ground Center, Eglin Air Force Base, Florida
Rpt No. AFGC-TDR-62-19, DIFFERENCE SCHEME FOR AXISYMMETRIC IMPACT PROBLEM. Qtrly progress rpt no. 4, Mar 62, 24p. incl illus., tables.

A numerical scheme which has been successfully employed for two-dimensional hydrodynamics is extended to the axisymmetric viscoplastic equations governing the hypervelocity impact phenomenon. Computing procedures are outlined which are complete enough for interior regions of the medium. The formulation must be further developed, however, to allow for such contingencies as free boundaries, interior empty cells and the axis of symmetry before a computing code can be written for the impact problem.

1. Impact shock
2. Hypervelocity projectiles
- I. AFSC Project 9860
- II. Contract AF 08(635)-1713
- III. General Electric Company, King of Prussia, Pa.
- IV. Riney, T. D.
- V. Quarterly Progress Report No. 4
- VI. In ASTIA collection

Air Proving Ground Center, Eglin Air Force Base, Florida
Rpt No. AFGC-I DR-62-19, DIFFERENCE SCHEME FOR AXISYMMETRIC IMPACT PROBLEM. Qtrly progress rpt no. 4, Mar 62, 24p. incl illus., tables.

A numerical scheme which has been successfully employed for two-dimensional hydrodynamics is extended to the axisymmetric viscoplastic equations governing the hypervelocity impact phenomenon. Computing procedures are outlined which are complete enough for interior regions of the medium. The formulation must be further developed, however, to allow for such contingencies as free boundaries, interior empty cells and the axis of symmetry before a computing code can be written for the impact problem.

1. Impact shock
2. Hypervelocity projectiles
- I. AFSC Project 9860
- II. Contract AF 08(635)-1713
- III. General Electric Company, King of Prussia, Pa.
- IV. Riney, T. D.
- V. Quarterly Progress Report No. 4
- VI. In ASTIA collection

Air Proving Ground Center, Eglin Air Force Base, Florida
Rpt No. AFGC-TDR-62-19, DIFFERENCE SCHEME FOR AXISYMMETRIC IMPACT PROBLEM. Qtrly progress rpt no. 4, Mar 62, 24p. incl illus., tables.

A numerical scheme which has been successfully employed for two-dimensional hydrodynamics is extended to the axisymmetric viscoplastic equations governing the hypervelocity impact phenomenon. Computing procedures are outlined which are complete enough for interior regions of the medium. The formulation must be further developed, however, to allow for such contingencies as free boundaries, interior empty cells and the axis of symmetry before a computing code can be written for the impact problem.

1. Impact shock
2. Hypervelocity projectiles
- I. AFSC Project 9860
- II. Contract AF 08(635)-1713
- III. General Electric Company, King of Prussia, Pa.
- IV. Riney, T. D.
- V. Quarterly Progress Report No. 4
- VI. In ASTIA collection

Air Proving Ground Center, Eglin Air Force Base, Florida
Rpt No. AFGC-I DR-62-19, DIFFERENCE SCHEME FOR AXISYMMETRIC IMPACT PROBLEM. Qtrly progress rpt no. 4, Mar 62, 24p. incl illus., tables.

A numerical scheme which has been successfully employed for two-dimensional hydrodynamics is extended to the axisymmetric viscoplastic equations governing the hypervelocity impact phenomenon. Computing procedures are outlined which are complete enough for interior regions of the medium. The formulation must be further developed, however, to allow for such contingencies as free boundaries, interior empty cells and the axis of symmetry before a computing code can be written for the impact problem.

1. Impact shock
2. Hypervelocity projectiles
- I. AFSC Project 9860
- II. Contract AF 08(635)-1713
- III. General Electric Company, King of Prussia, Pa.
- IV. Riney, T. D.
- V. Quarterly Progress Report No. 4
- VI. In ASTIA collection